

Effect of pH value on effectiveness of biopolymer-based treatment of bauxite mine slurry

Jianping Meng¹, Shanmei Li¹, Rongtao Yan¹, Changfu Wei^{1,2}

¹ Guangxi Key Laboratory of Geomechanics and Geotechnical Engineering, Guilin University of Technology, Guilin, Guangxi 541004, China

² State Key Laboratory of Geomechanics and Geotechnical Engineering, Institute of Rock and Soil Mechanics, Chinese Academy of Sciences, Wuhan, Hubei 430071, China

Corresponding author: cfwei@whrsm.ac.cn (Changfu Wei)

Abstract: Effective dehydration and flocculation of mine slurries or sludge is important for nonferrous metal industries and environmental engineering. However, the mechanisms for the flocculation of slurry remain largely unclear. This paper presents the results of a series of flocculation tests, which was conducted on the slurry suspensions treated by xanthan gum (flocculant) at different pH values. It is shown that the settlement rate of mine slurry particles can be accelerated by adding xanthan gum, and the maximum sedimentation rate was obtained at a pH value of 5.9, and the final volume of flocs is significantly increased due to the addition of the flocculant. In addition, the settlement rates of xanthan gum-treated slurry suspensions at the pH values of 3, 5 and 7 decrease slightly compared with the reference slurry suspensions with pH=5.9, and the slurries remained stable as suspensions at the pH value of 9 and 11. The zeta potential measurement and SEM image analysis show that flocculation occurs primarily due to electrostatic attraction between slurry particles and the flocculants, and the bridging effect between the carboxylic groups in the side chains of xanthan gum molecule and the suspension particles.

Keywords: pH, biopolymer, xanthan gum, bauxite mine slurry, flocculation

1. Introduction

Aluminum, the second largest metal after steel, plays an important role in the national economic development (Power et al., 2011). The demand for aluminum around the world has been growing quickly as a result of rapid industrialization and urbanization process during the past decades (Bonal et al., 2021). Bauxite ore is the main source for the production of alumina from which the metallic aluminum is extracted (Evans, 2016). The Bayer process is traditionally one of the methods to produce alumina. During the Bayer flotation process of bauxite ore, not only large amounts of bauxite ore can be extracted, but also a great deal of mine slurries are generated (Yang et al., 2009). It is reported that 0.8 to 1.0 tons of dry mine slurry or 1.0 to 2.5 tons of wet mine slurry are produced per ton of alumina extracted (Wu, 2021). According to statistical data, an alarmingly huge volumes of fine tailings, exceeding 20 billion tons, had been generated in China by the end of 2016 (Wang et al., 2016). In addition, as the high grade mineral resources are consumed in large amount, exploitation of low grade mineral resources has gradually become normal, thus leading to more and more production and accumulation of fine tailings (Jones et al. and Boger, 2012; Wang et al., 2014).

Traditionally, these bauxite mine slurries are discharged into a thickener, where solid-liquid separation is carried out under the action of chemical reagents, and then the settled slurry particles are pumped into the tailings ponds for storage by long distance pipelines (Wu et al., 2021; Ou et al., 2019). These coarse particles in the tailings ponds can precipitate quickly due to gravity. However, the fine slurry particles, with the particle size range typically less than about 10 μm and $d_{50}=0.06\text{mm}$ (Ou et al., 2020), are constantly in suspension without settlement for several decades or even longer time due to ultrafine sizes, resulting in high specific surface areas and strong colloidal interactions between particles

(Wang et al., 2014; Pal et al., 2011; Divakaran et al., 2001). The disposal of bauxite mine slurry not only entails a large amount of land resources, but also may form a potential threat to human safety and the ecological environment, such as slurry leakage accidents or tailing dam failures, especially in karst regions (Cheng et al., 2017; Wang et al., 2014). It has been reported that the tailing dam failures or tailing slurry leakages have generated serious effects, such as polluting the surface and groundwater, and flooding the downstream farmlands and villages (Ou et al., 2020; Wang et al., 2014). Therefore, discharging the mine slurry to tailings ponds for storage is no longer a long-term effective and safe slurry management strategy (Wang et al., 2014). The effective dehydration and disposal of bauxite mine slurry have become a challenge for mining companies.

Extensive research has been performed to accelerate the settlement of mine slurry particles, including electrophoresis, vacuum preloading, and chemical reagent additions (Ei-Shall and Zhang, 2004; Marie et al., 2021; Hogg, 2000; Ou et al., 2019, 2020). It is commonly believed that coagulation and flocculation of fine particles by adding appropriate chemical reagents are an important procedure for solid-liquid separation (Salehizadeh and Yan, 2014; Salehizadeh and Shojaosadati, 2001; Hogg, 2000). In general, flocculants can be split into three categories depending on their origin. Namely, inorganic flocculants, such as all kinds of aluminum and iron salts; synthetic organic flocculants, such as polyacrylamide and its derivatives; natural polymeric and microbial flocculants, such as chitosan, lignin, xanthan gum, and guar gum (Salehizadeh et al., 2018; Okaiyeto et al., 2016; Salehizadeh and Shojaosadati, 2001).

It is reported that inorganic or organic flocculants, especially polyacrylamide and its derivatives, have been used as flocculants in the solid-liquid separation of the mine slurry treatment. But, they have also brought about some serious environmental hazard and health risk (Okaiyeto et al., 2016; Rudén et al. 2004; Salehizadeh and Yan, 2014; Moghal et al., 2021; Peng et al., 2019). It is generally believed that these aluminum salts have a tendency to cause Alzheimer's disease (Campbell, 2002; Banks et al., 2006; Farrokhpay et al., 2021). Polyacrylamide, a water soluble polymer formed by polymerization of acrylamide monomer, is not readily degradable. Therefore, acrylamide monomer is considered as a carcinogen (Rudén, 2004; Salehizadeh et al., 2018). In contrast, polysaccharide biopolymers are particularly attractive as material sources due to their biodegradability, nontoxicity, environmental friendliness (Salehizadeh et al. 2018; Grenda et al., 2017). They have been considered as a feasible alternative to inorganic and organic synthetic flocculants in industrial application (Okaiyeto, 2016). Since the flocculating properties of biopolymers are understood, much attention has been paid to the research of the physicochemical factors impacting the flocculation activity (Brunchi et al., 2016; Li et al., 2014; Labille et al., 2005). Among all the factors affecting the flocculation effectiveness, it is generally believed that pH value of the suspension is considered to be one of the most important factors (Okaiyeto et al., 2016; Hogg 2000; Salehizadeh and Yan 2014; More et al., 2014; Ho et al., 2022). The effect of pH values on the flocculation effect of biopolymers has been evaluated by some scholars. Feng et al. (2017) showed that the flocculation velocity of quartz suspension treated by chitosan (a flocculant) was greatly influenced by the pH value, and the largest floc volume was obtained at pH of 9. Guibal et al. (2005) conducted a series of flocculation tests of mercury recovery with chitosan by sorption, and the results indicated that the doses required were significantly lower when the pH of the suspension was very low. However, the chitosan is soluble only in dilute hydrochloric or acetic acid solutions but not in water or concentrated organic solvents. Hence, its widespread application is restricted.

A large number of researches indicate that bioflocculants can be effectively used to treat kaolinite clay suspensions with a wide range of pH values. Gao et al. (2009) showed that the bioflocculant MBF4-13 from *Rothia* sp was effective for the flocculation of kaolin clay suspensions in the pH values of 1-13, with the maximum activity archived at pH 7-9. Experimental study by Luo et al. (2014) indicated that the bioflocculant MBF-6 produced by *Klebsiella pneumoniae* flocculating rate was over 80% in the pH values of 3-11, and the highest flocculating rate was achieved in a pH of 7. Similar results were obtained by Zulkeflee et al. (2012) who found that the flocculating activity of bioflocculant produced by *Bacillus* spp UPMB13 on kaolin suspension was influenced significantly by the a pH value, ranging from 4 to 8, the optimal pH value is pH 5 and pH 6. He et al. (2010) showed that the flocculating activity of bioflocculant HBF-3 in the kaolin particles was over 80% in the pH value of 3 to 11. The experimental conducted by Rajab Aljuboori et al. (2013) indicated that bioflocculant IH-7 from *Aspergillus flavus* had

high flocculating rate in kaolin suspension over the pH range of 3-7, and the flocculating rate decreased gradually in the pH values of 7-8. The experimental results conducted by Yim et al. (2007) indicated that the flocculating activity of p-KG03 produced by a *Gyrodinium impudicum* in kaolin suspension was effective in the pH value of 3 to 6. It was believed that the charged properties of polymers depend on the pH value of suspensions (Okaiyeto et al., 2016; Ho et al., 2022). Although numerous studies on the flocculating activity have been performed, these studies were performed on ideal slurries suspensions (focus mainly on kaolinite or quartz suspensions), and little attention was paid to fine mine slurries. The main objective of this paper is to explore the effect of the pH value on the effectiveness of biopolymer-based treatment of bauxite mine slurry. To this end, a series of flocculation tests is carried out by using xanthan gum as flocculant under five pH values (3, 5, 7, 9 and 11, respectively). Then, the effectiveness of flocculation is evaluated based on flocculation rate and floc-size distribution. The surface morphology and structure of the flocs are characterized by virtue of scanning electron microscopy.

2. Materials and methods

2.1. Slurry samples

The Bauxite mine slurry used in this test was sampled from the 2# washing ore site of Aluminum Industry Company of China Limited, Guangxi Branch. The mineralogical and chemical compositions of solid slurry were determined by using an X-ray diffractometer (X' Pert PRO Powder, PANalytical, Netherlands) and X-ray fluorescence spectroscopy (ZSX Primus II, Rigaku Corporation, Japan), respectively. The surface area was measured by using specific surface and aperture analyzer (JW-BK200C, JWGB SCI. & THCH, China). The spectrogram of mineralogical composition is shown in Fig.1, indicating that quartz, kaolinite, illite, and vermiculite are the primary mineralogical components. The basic physical properties and chemical compositions of the mine slurry are given in Table 1.

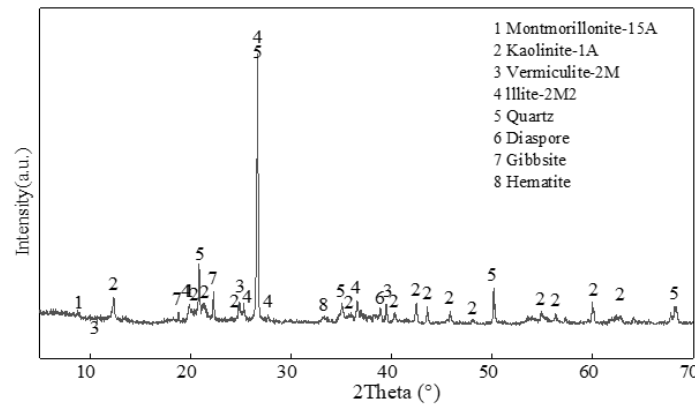


Fig. 1. Mineralogical composition spectrogram of mine slurry

Table 1. Physical properties and chemical compositions of the tested mine slurry

Physical properties			Chemical compositions	
Property	Value	Units	compositions	Percentage
Specific gravity	2.6	—	SiO ₂	33.7
Water content	258	%	Al ₂ O ₃	31.3
Specific surface area	31.5	m ² /g	Fe ₂ O ₃	16.3
natural pH	6.7	—	TiO ₂	1.6
Zeta potential of slurry at pH 6.7	-18.1	mV	K ₂ O	1.4
Liquid limit	65.6	%	CaO	0.5
Plastic limit	40.1	%	Na ₂ O	0.2
Plastic index	25.5	%	MgO	0.9

2.2. Chemical reagents

The chemical reagents used in this study include xanthan gum (flocculant), hydrochloric acid, potassium chloride and sodium hydroxide. The xanthan gum, an anionic polysaccharide based biopolymer, with molecular weight probably about 2 million (Nugent et al., 2009), was purchased from Shanghai Yuan Ye Biotech Co., Ltd, and used as a flocculant for bauxite mine slurry flocculation tests. The backbone structure of xanthan gum is mainly composed of two repeating glucose units, linked to each other by glycosidic bond through β (1 \rightarrow 4). The side chain comprise three linked monosaccharides units. Namely, two mannose units and one glucuronic units. The pyruvate group and acetate group are linked to the two mannose units, respectively. It is reported that the existence of the acetate and pyruvate in the side chains is the main reason why molecules are charged (Chatterji et al., 1981). The chemical structure is schematically represented in Fig. 2 (Abu Elella et al. 2021). As Fig. 2 shows, there exist a large number of hydroxyl and carboxylic group in the chemical structure (Nsengiyumva and Alexandridis, 2022). The xanthan gum molecules usually exhibit double helix structure as these functional groups interact with each other, and conformation transition in aqueous solutions, from ordered state to disorder state, is controlled by external conditions, such as ionic strength and pH of suspensions (Petri, 2015; Brunchi et al., 2016), resulting to influence the xanthan gum properties.

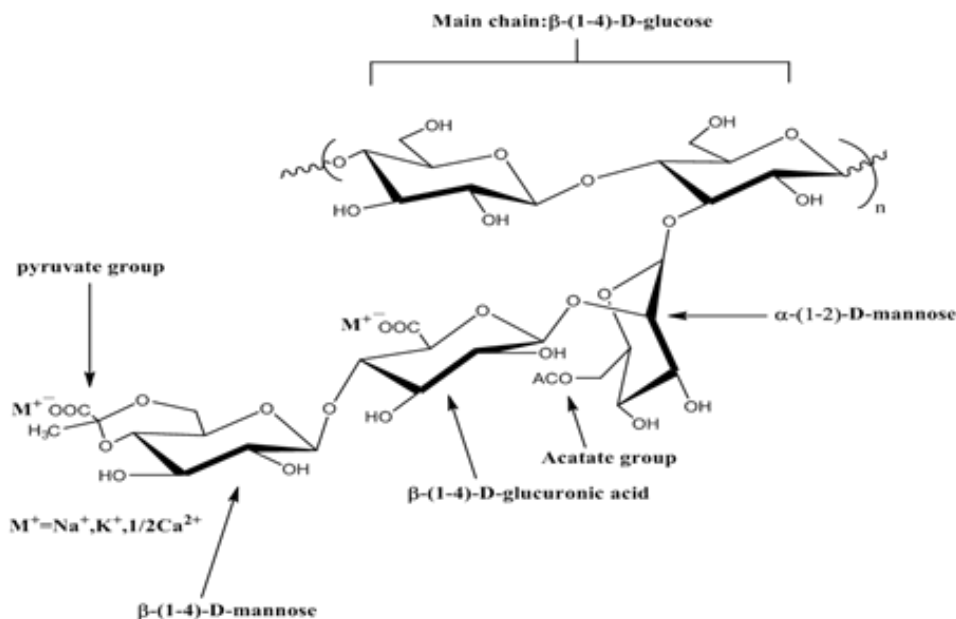


Fig. 2 Molecular structure of Xanthan gum (replotted after Abu Elella et al. (2021))

Hydrochloric acid, potassium chloride and sodium hydroxide were purchased from Shanghai Macklin Biotechnology Co., Ltd. The hydrochloric acid and sodium hydroxide were used to adjust the pH value of the mine slurry, while potassium chloride was used for the electrolyte background solution in the zeta potential measurements. All the chemical reagents were analytically pure and used immediately.

2.3. Mine slurry and biopolymer solution preparations

To minimize the influence of dissolved ions on flocculation, the mine slurry was first filtered by using a vacuum filter, then oven dried, and finally crushed by a grinder into a powder. The particle-size distribution of the powder was determined by using Malvern particle-size analyzer (Mastersizer 3000, Malvern, UK) and the results were displayed in Fig. 3. The artificial slurry suspensions were prepared with the same concentration of the bauxite mine slurry on site, which was about 9% in percentage of the dry weight of mine slurry particles to the total weight of slurry suspensions. To this end, 9.06g dried mine slurry powder was mixed with 91.56g distilled water (pH=5.6) in a beaker, and then stirred by using the magnetic stirring method at room temperature for 1 hour to ensure the clay powder evenly distributed.

Three parts of the xanthan gum powders were weighed, and they were 0.324g, 0.504g and 0.684g respectively. then dissolved in 180g of distilled water (pH=5.6) and stirred for 6 hours by using the magnetic stirring method at room temperature. The prepared xanthan gum solutions concentrations are 0.18, 0.28 and 0.38 wt%, respectively. To prevent biological degradation, all the prepared xanthan gum solutions were used immediately in the experiments.

2.4. Flocculation tests

Flocculation tests were conducted on the prepared mine slurry at room temperature, in a 100 milliliter glass cylinder, to evaluate the influence of the pH value on the effectiveness of the biopolymer treatment of bauxite mine slurry. Before the test, the pH values of the prepared suspensions were targeted to 3, 5, 7, 9 and 11, respectively, by using analytical grade hydrochloric acid (0.01 m/l) and sodium hydroxide solutions (0.1 m/l). The prepared suspensions were stirred up and down for 3 minutes with a customized stirrer to ensure homogenization. Then, 5 ml prepared xanthan gum solutions was sucked with a high-accuracy pipette and added to the slurry suspensions, and stirred up and down four times. For comparison, flocculation tests were also performed on the slurry without xanthan gum.

2.5. Floc-size measurement

The particle-size distributions of the prepared bauxite mine slurry and flocs, taken from a depth of 1 cm below the soil-water interface after flocculation tests, were conducted with laser light scattering technology with Mastersizer 3000 (Malvern Zetasizer Nano, UK).

2.6. Zeta potential measurement

Zeta potentials (ZPs) of the crushed slurry powder and biopolymer-treated slurry were measured with a nanoparticle and Zeta potential analyzer (Malvern Panalyti, UK). The measurements were performed on the prepared mine slurry suspensions of 0.1 wt% in a 10⁻³ mol/l KCl electrolyte background solution. For the crushed slurry powder, the pH value was regulated with 0.01 m/l hydrochloric acid and 0.1 m/l sodium hydroxide. Each measurement was triplicated, and the average was used as the final measured value.

2.7 Scanning Electron Microscopy

Surface morphology of the prepared slurry particles and their flocs was analyzed by scanning electron microscopy (Gemini SEM 300, UK). The slurry suspension and flocs were first dried by using the freeze-drying methods, and then placed on a SEM platform and covered by conductive carbon black for surface morphology and structure observations.

3. Results and discussion

3.1 Slurry powder characterization

The particle-size distribution of the crushed bauxite mine slurry powder is showed in Fig. 4. It can be seen that the particle sizes range from ~0.2 μm to 120 μm , with d50 and d90 of approximately 27 μm and 72 μm , respectively. The SEM image of the surface morphology of slurry particles is shown in Fig. 4, indicating that the mine slurry is mainly composed of fine particles, and most of the particles have a lamellate plate shape, with very rough edges. The surface structure is very complicated and fragmented. In addition, the sizes of pores are very different.

3.2 Settlement rates

As well recognized, the sedimentation of a suspension includes three stages, i.e., flocculation stage, settlement stage, and consolidation stage. The settlement rates are defines as the slope of the linear portion of the mud-line settling curve in the settlement stage. The effect of the pH values on the sedimentation of the xanthan gum-treated mine slurries after 7-days settlement is demonstrated in Fig. 5, where the interfaces between supernatant and floc can be clearly seen. The raw suspension is the simple mixture of crushed mine slurry powder and distilled water (pH=5.6). The suspension with a pH

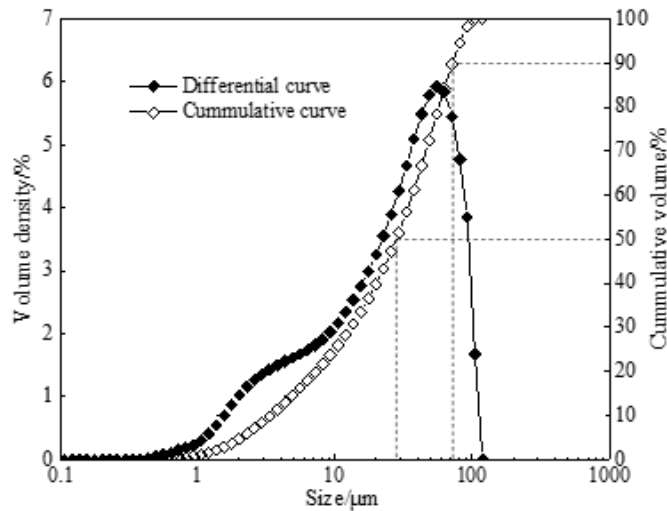


Fig. 3. Particle size distribution of mine slurry



Fig. 4. The SEM images of mine slurry

value of 5.9 is a reference, which is made by adding a certain amount of xanthan gum (2097 g gum/ton solid) to the raw suspension. The other suspensions are prepared by adjusting the pH values of the reference suspension (pH=5.9) to the targeted values of 3, 5, 7, 9, and 11, respectively. Comparison between the raw and reference suspensions indicates that addition of xanthan gum can increase sedimentation volume, which is the total volume of floc. When the pH value ranges from 3 to 7, the sedimentation volume is slightly influenced by the pH value. At higher pH values, however, the sedimentation volume increases significantly, so that the slurry remains in a suspending state for a long time.

Fig. 6 shows the temporal variations of the interfacial height of the mine slurries with different pH values at mass ratios (denoted by mR hereinafter) of 993, 1545 and 2097 g gum/ton solid, respectively. Here, the interfacial height refers to the height of the interface between supernatant and floc, and mR is defined as the weight (gram) of added xanthan gum per ton of dried slurry solid.

Clearly, three stages can be identified, i.e., flocculation, settlement and consolidation. It can be seen that the final interfacial height of the suspension generally increases with the increase in the mass ratio of the slurry suspension. At high pH values (9 and 11), the interfacial height remains practically unchanged as time elapses, for all three mass ratios. Meanwhile, it is obvious in Fig. 6 that the temporal variations of interfacial height of mine slurries with pH values of 5.9, 7, 9 and 11 at different mass ratios

are similar, except the pH=3 and pH=5. As the pH value increases from 3 to 7, the final interfacial height increases for the mass ratio of 993 g gum/ton solid, and decreases for the mass ratios of 1545 and 2097 g gum/ton solid. In general, the rate of settlement increases with the pH value, though it is very slightly influenced by the pH value less than 6.

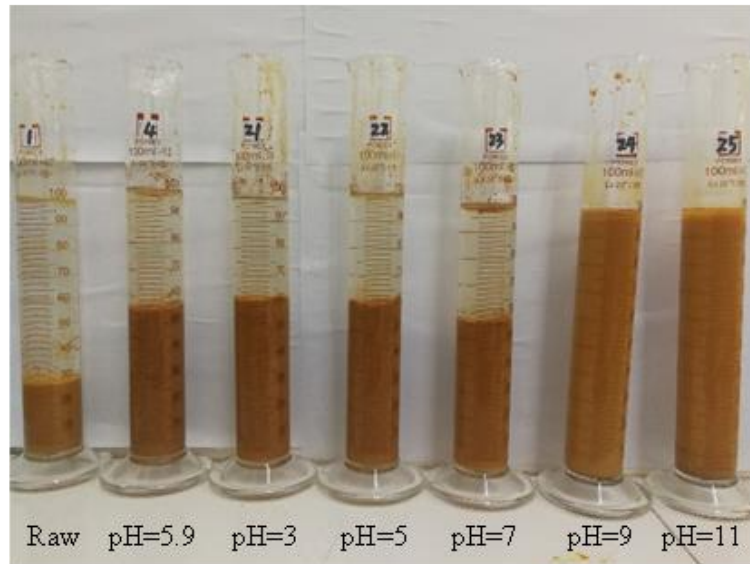


Fig. 5. Effect of pH on the flocculation of xanthan gum-treated mine slurry after 7-days settlement

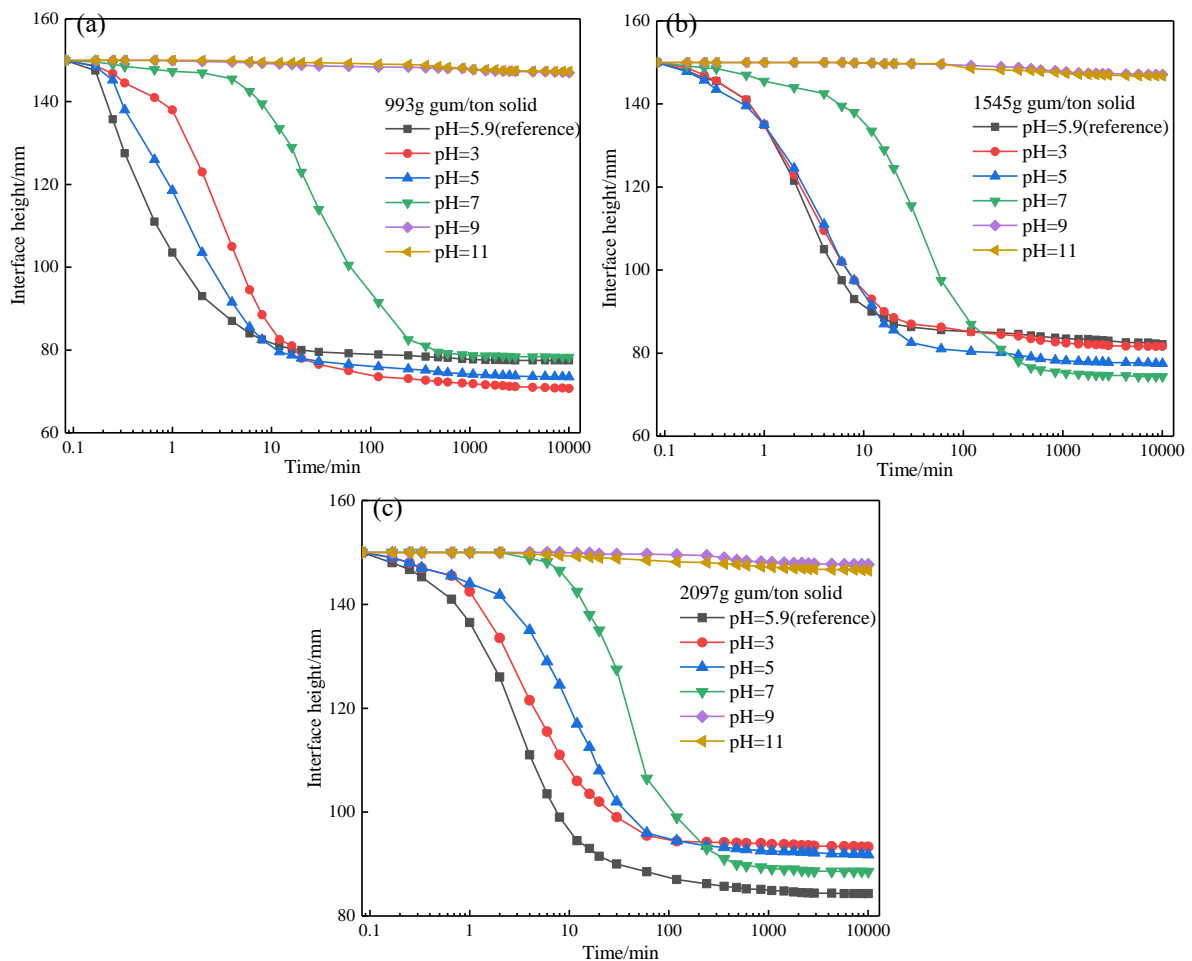


Fig. 6. Temporal variations of interfacial height of mine slurries with different pH values at mass ratios of (a) 993 g gum/ton solid, (b) 1545 g gum/ton solid, and (c) 2097 g gum/ton solid respectively

3.3. Floc size distribution

The flocs-size distributions at different pH values are compared in Fig. 7, indicating that xanthan gum can remarkably influence the particle-size distribution of the slurry suspensions. The effect of pH value is significant on the flocs-size distribution of the slurry treated with low concentrated xanthan gum, while insignificant for those treated with medially and highly concentrated xanthan gum. The particle sizes of the raw slurry are widely distributed, following a normal distribution, and the content of large particles significantly increases after the treatment of xanthan gum for all the three mass ratios. The particle sizes of raw slurry range from 0.8 μm to 110 μm . For the slurry with mR of 993 g gum/ton solid, the number of particles larger than 50 μm increases significantly at the pH values less than 9; at the pH value of 9 and 11, the number of particles between 5 and 40 μm , and between 4 and 37 μm respectively, increases significantly, whereas the number of particles with other sizes decreases. For the slurries with mass ratios mR of 1545 g gum/ton solid, the number of large particles increases significantly with the pH value. However, For the slurry with mR of 2097 g gum/ton solid, the number of particles larger than 50 μm increases significantly at the pH values less than 9; at the pH value of 9 and 11, the number of particles between 4.5 and 40 μm , and between 8 and 50 μm respectively, decreases observably, whereas the number of particles with other sizes increases.

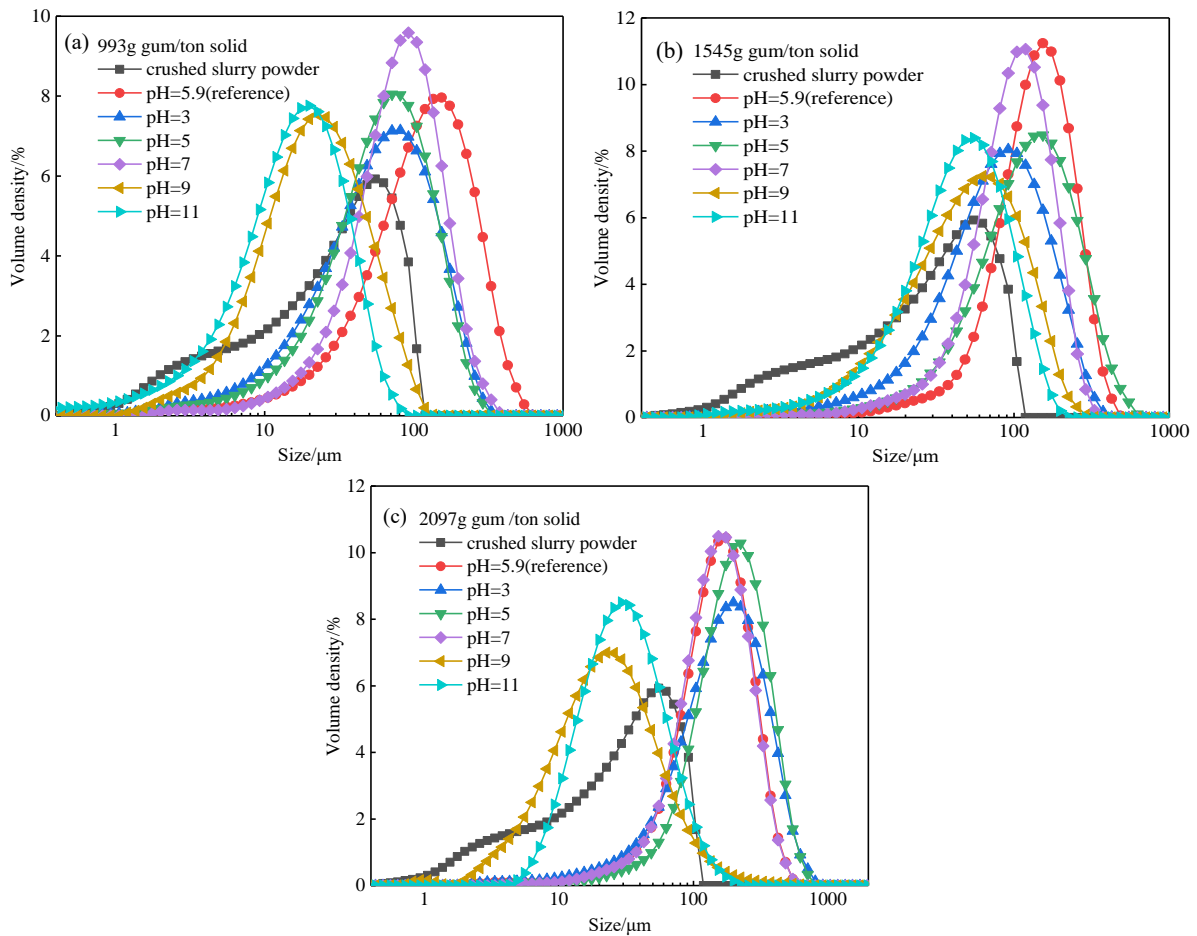


Fig. 7. Particle diameter of flocs after flocculation completed (a) 993 g gum/ton solid, (b) 1545 g gum/ton solid, and (c) 2097 g gum/ton solid respectively

4. Discussion

Fig. 1 reveals that the primary mineralogical components of the tested bauxite mine slurry are quartz, kaolinite, illite, and vermiculite. It has been determined that the particles of original slurry suspension taken from the washing ore site before draining into the thickener, are mainly negatively charged, with a zeta potential of -18.1 mV at the natural pH value of 6.7. As can be seen in the Fig. 2, there are a large

number of reactive functional groups such as hydroxyl and carboxylic groups on the molecular structure of xanthan gum. Xanthan gum is soluble in hot or cold water, usually exhibiting a helical configuration (Nsengiyumva and Alexandridis, 2022; Brunchi et al., 2016). When the pH values of the medium change, the carboxylic groups on the xanthan gum molecule become protonated or deprotonated, resulting in the conformational transition and providing binding sites to adsorb suspended slurry particles (He et al., 2010). Also, when the mine slurry particles are very close to xanthan molecules, the hydroxyl groups have a tendency to form hydrogen bonds with slurry particles, since the mine slurry particles contains various types of clay minerals.

The adsorption effect is schematically shown in Fig. 8 (The golden circles represent soil particles, and the blue curves represent xanthan gum chains). In other words, the side chains and the backbones of xanthan gum molecules can adsorb suspended particles, resulting in the flocculated structure of the slurry suspension treated by xanthan gum. Hence, it is the interaction between xanthan gum molecules and fine particles that promotes the formation of gelatinous three-dimensional network with a large number of pores, as clearly shown in Fig. 9(a). Obviously, the aggregation (dark blue line) of soil particles can be seen. To exhibit the adsorption of particles, we adopted a mass ratio of 100 g gum / 1g solid in mixing the xanthan gum and the raw slurry, and took the SEM image, which is shown in Fig. 9(b). It can be clearly seen that slurry particles are adsorbed onto the xanthan gum molecule. Apparently, the form of inter-particle contacts has been changed by the added xanthan gum molecules. Indeed, before the addition of xanthan gum, the dominated contact modes of particles under gravity are mainly face to face contact (see Fig. 2). After the treatment of xanthan gum, however, the structure of the suspension is changed into a three-dimensional network. As a consequence, the pore sizes of the slurry increase due to the addition of xanthan gum, resulting in a significant increase of the volume of the xanthan gum-treated mine slurry (see Fig. 5).

Fig. 10 illustrates the variations of zeta potential with the pH value for various slurry suspensions. For the raw suspension, the variation of zeta potential with the pH value can be decomposed into three

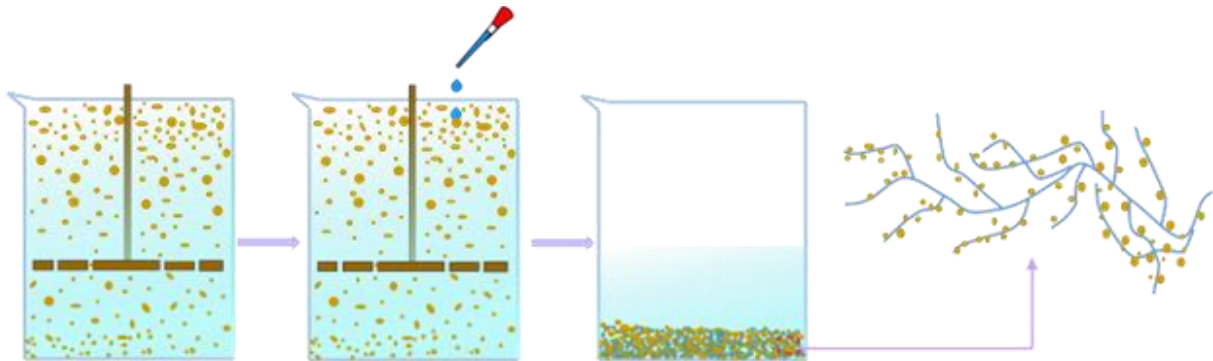


Fig. 8. Schematic illustration of flocculation mechanism

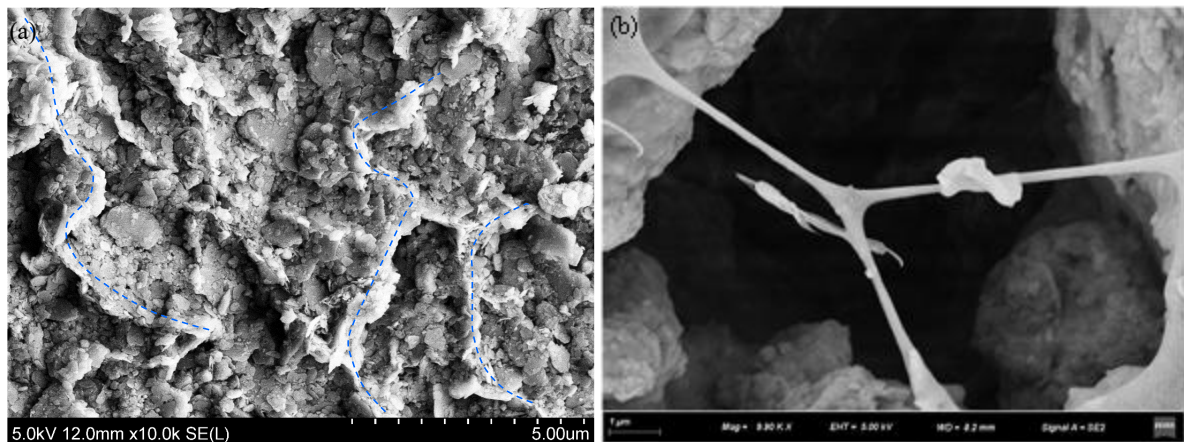


Fig. 9. SEM images of slurry structure. (a) Overall structure of xanthan gum-treated slurry; (b) particles adsorbed onto xanthan gum

stages. As the pH value increases, the zeta potential first increases slightly until pH=3; then, decreases dramatically until pH=4.4, fluctuates at pH values between 4.4 and 8.0, and decreases again until pH=10.8; finally, increases again. The fluctuation of zeta potential at pH values between 4.4 and 8.0 can be attributed to the variation of the charge density of pH-dependent hydroxyl groups at the particle edges. Clearly, the zero point of charge (ZPC) of the raw slurry is about 3.5. For the suspensions treated by xanthan gum, the zeta potential decreases constantly with the increase of pH value, and it is always negative. Sriprablom and Suphantharika (2022) showed that at a pH value ranging from 3 to 9, the zeta potential of xanthan gum solution is always negative.

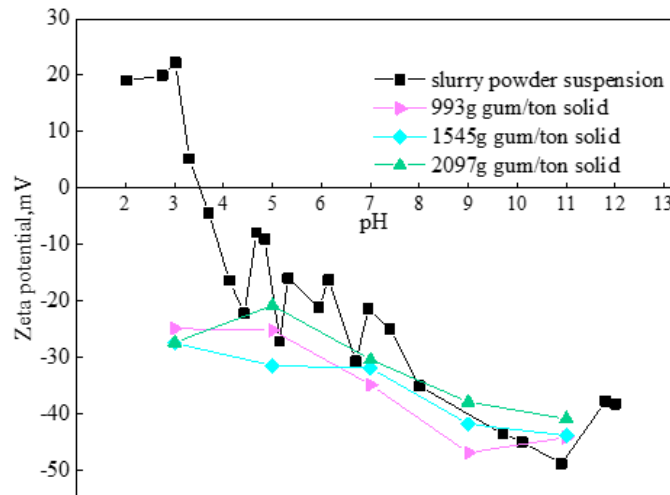


Fig. 10. Variation of zeta potential with pH value for various suspensions

As mentioned above, the slurry suspensions with pH values of 9 and 11 remain stable as flocculated suspensions, without significant settlement, even after being treated by xanthan gum. This can be partially attributed to the fact that the numbers of the surface charges of the particles in these suspensions are large at pH=9 and pH=11. In addition, the xanthan gum molecules in a solution are generally negatively charged, potentially increasing the zeta potential of the suspension. Indeed, the zeta potential at the pH values between 9 and 11 is down to -40mV, implying that strong electrostatic repulsive forces exist among slurry particles, so that no significant settlement occurs in the suspension (Brunchi et al., 2016; Morariu et al., 2012). Therefore, the variations of interfacial height of slurries with pH=9 and pH=11 at different mass ratios of xanthan gum to solid are similar. Fig. 10 also shows that at the pH values below 3.5, the raw slurry suspension particles are positively charged. Noticeably, the zeta potential of xanthan gum aqueous solution is negative in the pH value range from 3 to 9 (Sriprablom and Suphantharika, 2022). Therefore, at a pH value less 3.5, the electrostatic attraction interaction between the xanthan and slurry particles induces aggregation. When the pH values of the slurry suspensions are 5, the slurry particles are negatively charged. The carboxylic groups of the xanthan gum molecules dissociate into $-\text{COO}^-$ groups and hydrogen ion (Li et al., 2012; Dontsova and Bigham, 2005). It is also reported that the carboxylic groups become partially deprotonated at pH=5 (Brunchi et al., 2016), making the xanthan gum chains become partially flexible to cause more slurry particles to interact with the xanthan gum molecules by hydrogen bond to form larger flocs compared to that at pH=3, corresponding to the particle size distribution results of flocs (Fig. 7(a)). The increase of the xanthan gum added to the slurry suspensions leads to the formation of a weak network gel structure (Xiao et al., 2021), leading to inadequate binding sites for the slurry particles to form hydrogen bonds. Thus, the interaction between the slurry particles and the xanthan gum is mainly the electrostatic attraction between the xanthan gum and the positively charged edges of the slurry particles. On the other hand, the increase of the xanthan gum mass ratios can improve the viscosity of the slurry suspensions, reducing the settlement rate of the flocs. Hence the variations of interfacial height of slurry suspensions with pH=3 at 2097 g gum/ton solid are slightly greater than that with pH=5.

At the pH values between 4 and 7, the slurry suspensions can also become aggregated. On one hand, as the primary mineralogical compositions of the mine slurry, aluminum oxide and ferric oxide are

positively charged; on the other hand, the xanthan gum molecules in an aqueous solution is negatively charged at a pH value between 3 and 9 (Sriprablom and Supphantharika, 2022). Hence, electrostatic attractions occur between the xanthan gum molecules and slurry particles. In general, the molecular conformational transition of xanthan gum is affected by the pH value. Brunchi et al. (2016) reported that, at a pH value of 5 or 6, the carboxylic groups of the xanthan gum molecular became partially protonated or even completely deprotonated, resulting in the formation of $-\text{COO}^-$ groups on the side chains of xanthan gum molecules and the enhancement of the electrostatic repulsive forces between the side chains. As a consequence, the side chains of xanthan molecules expand and become flexible (Brunchi et al., 2016; Pan et al., 2020), resulting in more and more slurry particles are adsorbed onto the xanthan gum molecules. But, when the pH of the suspensions is 7, the xanthan gum chains become partially flexible, thus reducing the contact between the xanthan gum chains and slurry particles. Meanwhile, the zeta potentials of the flocs at pH=7 are between -34.9 mV and -30.4 mV (Fig. 10). The suspension was in a metastable state when the zeta potential of xanthan gum-treated mine slurry ranged from -30 mV to 30 mV (Brunchi et al., 2016). Therefore, the variations of interfacial height of slurry suspensions with pH=7 are slower than that with pH=5.9. But, the variations of interfacial height of slurries with pH=5.9 and pH=7 at different mass ratios of xanthan gum to solid are similar. When xanthan gum was added into the suspension, the settlement readily occurred. Based on our experimental results, the settlement rate is the fastest at a pH value of 5.9. The structure of the xanthan gum-treated slurry is shown in Fig. 11, indicating that a large number of fine particles are concentrated due to the gelation of xanthan gum.

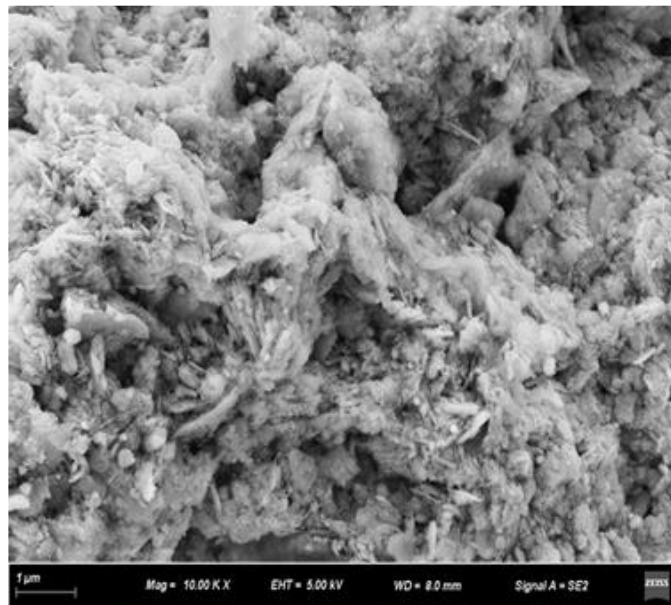


Fig. 11 SEM image of the xanthan gum-treated slurry with mass ratio of 1545 g gum/t solid at pH=5.9

4. Conclusions

In this research, a series of experiments was performed on the bauxite mine slurry suspensions, with or without being treated by xanthan gum, to explore the effect of pH value on the flocculation effectiveness of xanthan gum. The zeta potential measurement and SEM analysis were conducted to clarify the underlying mechanisms for xanthan gum-induced flocculation.

It is shown that the flocculation of bauxite mine slurry can be accelerated by adding xanthan gum, and the final volume of flocculation is significantly increased by the added flocculants. In addition, the slurries remained stable as suspensions at the pH value of 9 and 11, independent of the amount of xanthan gum added. It is found that the ZPC (zero point of charge) of raw slurry powder is about 3.5. The settlement rates of xanthan gum-treated slurry suspension with the pH values of 3, 5 and 7 decrease slightly compared with the reference slurry suspensions with pH=5.9.

Two possible mechanisms account for the flocculation of the mine slurry suspensions. One is the electrostatic interaction between the particles and the xanthan gum molecules at low pH values.

Another is the bridging effect between the carboxylic groups in the side chains of xanthan gum molecule and the suspension particles, which can strengthen the contact between the slurry particles and xanthan gum molecules and promote the formation of hydrogen bond.

Acknowledgment

This study was supported by the National Natural Science Foundation of China under Grants No. 51939011 and No. 52268055.

References

- ABU ELELLA, M. H., GODA, E. S., GAB-ALLAH, M. A., HONG, S. E., PANDIT, B., LEE, S. H., GAMAL, H., REHMAN, A. U., YOON, K. R., 2021. *Xanthan gum-derived materials for applications in environment and eco-friendly materials: A review*. Journal of Environmental Chemical Engineering. 9 (1) 104702.
- Banks, W. A., Niehoff, M. L., Drago, D., ZATTA, P., 2006. *Aluminum complexing enhances amyloid β protein penetration of blood-brain barrier*. Brain Research. 1116 (1) 215–221.
- BRUNCHI, C. E., BERCEA, M., MORARIU, S., DASCALU, M., 2016. *Some properties of xanthan gum in aqueous solutions: effect of temperature and pH*. Journal of Polymer Research. 23 (7) 123.
- BONAL, N. S., PRASAD, A., VERMA, A. K., 2021. *Effect of microbial biopolymers on mechanical properties of bauxite residue*. KSCE Journal of Civil Engineering. 25 (7) 2437–2450.
- CAMPBELL, A., 2002. *The potential role of aluminum in Alzheimer's disease*. Nephrology Dialysis Transplantation. 17 17–20.
- CHATTERJI, J., BORCHARDT, J. K., 1981. *Applications of water-soluble polymers in the oil field*. Journal of Petroleum Technology. 33 (11) 2042–2056.
- CHENG, F., SU, X. Z., ZHOU, J. J., GUO, S., Q., 2017. *Leakage mechanism and comprehensive prevention control technology of tailing pond in karst areas*. Carsologica Sinica. 36 (2) 242–247.
- DIVAKARAN, R., SIVASANKARA, PILLAI, V. N., 2001. *Flocculation of kaolinite suspensions in water by Chitosan*. Water Res. 35 (16) 3904–3908.
- DONTSOVA, K. M., BIGHAM, J. M., 2005. *Anionic Polysaccharide Sorption by Clay Minerals*. Soil Science Society of America Journal. 69(4) 1026.
- EI-SHALL, H., ZHANG, P., 2004. *Process for dewatering and utilization of mining wastes*. Minerals Engineering. 17 (2) 269–277.
- EVANS, K., 2016. *The History, Challenges, and New Developments in the Management and Use of Bauxite Residue*. Journal of Sustainable Metallurgy. 2 (4) 316–331.
- FENG, B., PENG, J. X., ZHU, X. W., HUANG, W. F., 2017. *The settling behavior of quartz using chitosan as flocculant*. Journal of Materials Research and Technology. 6 (1) 71–76.
- FARROKHPAY, S., FILIPPOV, L. X., FORNASIERO, D., 2021. *Flotation of Fine Particles: A Review*. Mineral Processing and Extractive Metallurgy Review. 42 (7) 473–483.
- GUIBAL, E., TOURAUD, E., ROUSSY, J., 2005. *Chitosan interactions with metal ions and dyes: dissolved-state versus solid-state application*. World J Microb Biotechnol. 21 913–920.
- GREYDA, K., ARNOLD, J., GAMELAS, A. F., RASTEIRO, M. G., 2017. *Environmentally friendly cellulose-based polyelectrolytes in wastewater treatment*. Water Science and Technology. 76 (6) 1490–1499.
- GAO, Q., ZHU, X. H., MU, J., ZHANG, Y., DONG, X. W., 2009. *Using ruditapes philippinarum conglutination mud to produce bioflocculant and its applications in wastewater treatment*. Bioresource technology. 100 (21) 4996–5001.
- HE, J., ZOU, J., SHAO, Z., ZHANG, J., LIU, Z., YU, Z., 2010. *Characteristics and flocculating mechanism of a novel bioflocculant HBF-3 produced by deep-sea bacterium mutant Halomonas sp. V3a'*. World Journal of Microbiology and Biotechnology. 26 (6) 1135–1141.
- HO, Q. N., FETTWEIS, M., SPENCER, K. L., LEE, B. J., 2022. *Flocculation with heterogeneous composition in water environments: A review*. Water Research. 213 (15) 118147.
- HOGG, R., 2000. *Flocculation and dewatering*. International Journal of Mineral Processing. 58 223–236.
- JONES, H., BOGER, D. V., 2012. *Sustainability and waste management in the resource industries*. Industrial & Engineering Chemistry Research. 51 (30) 10057–10065.
- KONDURI, M. K. R., FATEHI, P., *Influence of pH and ionic strength on flocculation of clay suspensions with cationic xylan copolymer*, Colloids and Surfaces A. 530 (2017) 20–32.

- LABILLE, J., THOMAS, F., MILAS, M., VANHAVERBEKE, C., 2005. *Flocculation of colloidal clay by bacterial polysaccharides: effect of macromolecule charge and structure*. Journal of Colloid and Interface Science. 284 149–156.
- LI, H. J., CAI, T., YUAN, B., LI, R. H., YANG, H., LI, A. M., 2014. *Flocculation of both kaolin and hematite suspensions using the starch-Based flocculants and their floc properties*. Industrial & Engineering Chemistry Research. 54 (1) 59–67.
- LI, H. P., HOU, W. G., LI, X. Z., 2012. *Interaction between xanthan gum and cationic cellulose JR400 in aqueous solution*. Carbohydrate Polymers. 89 (1) 24–30.
- LUO, Z. S., CHEN, L., CHEN, C. H., ZHANG, W., LIU, M., HAN, Y., ZHOU, J. G., 2014. *Production and characteristics of a bioflocculant by klebsiella pneumoniae YZ-6 isolated from human saliva*. Applied Biochemistry and Biotechnology, 172 (3) 1282–1292.
- MARIE, J., BOURRET, J., GEFFROY, P. M., CHARTIER, T., BIENIA, M., CHALEIX, V., PICTON, L., SMITH, A., 2021. *Impact of bio-based binders on rheological properties of aqueous alumina slurries for tape casting*. Journal of the European Ceramic Society. 41 (11) 5593–5601.
- MOGHAL, A. A. B., VYDEHI, K. V., 2021. *State-of-the-art review on efficacy of xanthan gum and guar gum inclusion on the engineering behavior of soils*. Innovative Infrastructure Solutions. 6 (2) 1–14.
- MORE, T. T., YADAV, J. S. S., YAN, S., TYAGI, R. D., SURAMPALLI, R. Y., 2014. *Extracellular polymeric substances of bacteria and their potential environmental applications*. Journal of Environmental Management. 144 1–25.
- MORARIU, S., BRUNCHI, C. E., BERCEA, M., 2012. *The Behavior of Chitosan in Solvents with Different Ionic Strengths*. Industrial & Engineering Chemistry Research. 51 12959–12966.
- NUGENT, R. A., ZHANG, G., GAMBRELL, R. P., 2009. *Effect of exopolymers on the liquid limit of clays and its engineering implications*. Transportation Research Record. 2101 (1) 34–43.
- NSENGIYUMVA, E. M., ALEXANDRIDIS, P., 2022. *Xanthan gum in aqueous solutions: Fundamentals and applications*. International Journal of Biological Macromolecules. 216 583–604.
- OKAIYETO, K., NWODO, U. U., OKOLI, S. A., MABINYA, L. V., OKOH, A. I., 2016. *Implications for public health demands alternatives to inorganic and synthetic flocculants: bioflocculants as important candidates*. Microbiology Open. 5 177–211.
- OU, X. D., PENG, Y. S., HOU, K. W., SU, J., JIANG, J., 2019. *Experimental research on biochemical consolidation of bauxite tailings clay*. Arabian Journal of Geosciences. 12 (24) 1–10.
- OU, X. D., MO, P., JIANG, J., SU, J., PENG, Y. S., 2020. *Experimental study on solidification of bauxite tailing clay with quicklime and microorganism*. Chinese Journal of Geotechnical Engineering. 42 (4) 624–631.
- PAL, S., GHORAI, S., DASH, M. K., GHOSH, S., UDAYABHANU, G., 2011. *Flocculation properties of polyacrylamide grafted carboxymethyl guar gum (CMG-g-PAM) synthesised by conventional and microwave assisted method*. Journal of Hazardous Materials. 192 (3) 1580–1588.
- PAN, G., SHI, Q., ZHANG, G. F., HUANG, G. H., 2020. *Selective depression of talc in chalcopyrite flotation by xanthan gum: Flotation response and adsorption mechanism*, Colloids and Surfaces A. 600 124902.
- PETRI, D. F. S., 2015. *Xanthan gum: A versatile biopolymer for biomedical and technological applications*. Journal of Applied Polymer Science. 132(23): 42035.
- PENG, Y. S., JIANG, J., OU, X. D., QIN, J., X. 2019. *Investigating the Properties of Foamed Mixture Lightweight Soil Mixed with Bauxite Tailings as Filler*. Advances in Materials Science and Engineering. 12 (24) 1–10.
- POWER, G., GRÄFE, M., KLAUBER, C., 2011. *Bauxite residue issues: I. Current management, disposal and storage practices*. Hydrometallurgy, 108 (1-2) (2011) 33–45.
- RAJAB ALJUBOORI, A. H., IDRIS, A., ABDULLAH, N., MOHAMAD, R., 2013. *Production and characterization of a bioflocculant produced by Aspergillus flavus*. Bioresource Technology. 127 489–493.
- RUDÉN, C., 2004. *Acrylamide and cancer risk—expert risk assessments and the public debate*. Food and Chemical Toxicology. 42 (3) 335–349.
- SALEHIZADEH, H., YAN, N., 2014. *Recent advances in extracellular biopolymer flocculants*. Biotechnology advances. 32 1506–1522.
- SALEHIZADEH, H., SHOJAOSADATI, S. A., 2001. *Extracellular biopolymeric flocculants Recent trends and biotechnological importance*. Biotechnology Advances. 19 371–385.
- SALEHIZADEH, H., YAN, N., FARNOOD, R., 2018. *Recent advances in polysaccharide bio-based flocculants*. Biotechnology advances, 36(1) 92–119.

- SRIPRABLOM, J., SUPHANTHARIKA, M., 2022. *Influence of xanthan gum on properties and stability of oil-in-water Pickering emulsions stabilized by zein colloidal particles*. Journal of Food Measurement and Characterization. 16 2772-2781.
- XIAO, N. H., HE, W., ZHAO, Y., YAO, Y., XU, M. S., DU, H. Y., WU, N., TU, Y. G., 2021. Effect of pH and xanthan gum on emulsifying property of ovalbumin stabilized oil-in water emulsions. LWT-Food Science and Technology. 147 111621.
- WU, Z. Q., XU, K., WANG, Z. H., LI, S. H., JIANG, B. Y., 2021. *Soil-water separation property of bauxite mine slime*, Hydraulic and Civil Engineering Technology VI. 69 104-111.
- WANG, H. J., XUE, Y. Z., LEI, P. Q., 2016. *National Report on Conservation and comprehensive utilization of mineral resources*, Geological Press. Beijing.
- WANG, C., HARBOTTLE, D., LIU, Q. X., XU, Z. H., 2014. *Current state of fine mineral tailings treatment: A critical review on theory and practice*, Chinese Journal of Geotechnical Engineering. 58 113-131.
- YANG, H. Z., CHEN, C. P., PAN, L. J., LU, H. X., SUN, H.W., HU, X., 2009. *Preparation of double-layer glass-ceramic/ceramic tile from bauxite tailings and red mud*, Journal of the European Ceramic Society. 29 (10) 887-1894.
- YIM, J.H., KIM, S.J., AHN, S.H., LEE, H. K., 2007. *Characterization of a novel bioflocculant, p-KG03, from a marine dinoflagellate*. Gyrodinium impudicum KG03, Bioresource Technology. 98 (2007) 361-367.
- ZULKEFLEE, Z., ARIS, A. Z., SHAMSUDDIN, Z. H., YUSOFF, M. K., 2012. *Cation dependence, pH tolerance, and dosage requirement of a bioflocculant produced by Bacillus spp. UPMB13: Flocculation performance optimization through kaolin assays*. The Scientific World Journal. 1-7.